THE JOURNAL OF PHYSICAL CHEMISTRY C

ACS AUTHORCHOICE

pubs.acs.org/JPCC Article

Soft Selection Rules for Femtosecond Pump−Probe Vibrational Coherence Spectroscopy

Published as part of The Journal of Physical Chemistry virtual special issue "Josef Michl Festschrift".

Marcin Andrzejak, Grzegorz Mazur, Tomasz Skóra, and Piotr Petelenz*

Cite This: *J. Phys. Chem. C* 2020, 124, 23501−23510

Read Online

ACCESS | Metrics & More | Article Recommendations | Supporting Information

ABSTRACT: Persevering research efforts that seek to harness the potential of singlet fission to increase the efficiency of photovoltaic devices have recently focused on vibronic mechanisms that presumably underlie this process. The fundamental theoretical input needed for treating the transitions between the electronic states involved are the Franck−Condon parameters that govern the generation of the coherent vibrational wave packets emerging in the fission phenomenon and in the experiments performed for its investigation. Their calculation for triplet states is not commonly practiced, so they are usually simulated by their singlet counterparts. On the basis of the analysis of coherence flow descriptors, here we find the validity of this approximation questionable for subtle interpretative issues of femtosecond pump−probe vibrational spectroscopy where a slight difference in a mode's coherence power may have a pivotal role in assessing the mechanism of fission dynamics. In less sensitive instances, the approach is acceptably reliable at qualitative level, apart from a tendency to predict sporadic spurious coherences. Our methodology may lead to a potential tool for detecting those artifacts.

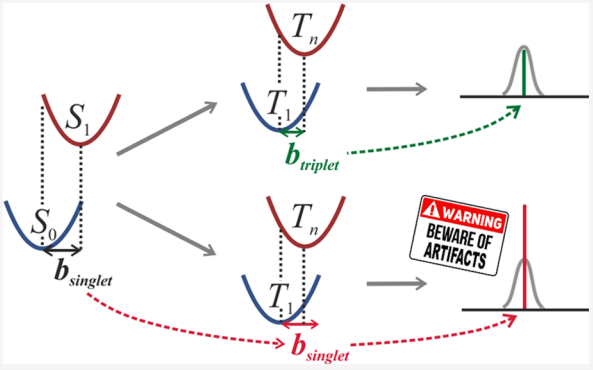

1. INTRODUCTION

Singlet fission (SF) continues to receive much interest in the recent literature[1−9] largely due to the putative application of this phenomenon to further increase the efficiency of optoelectronic devices by amplifying the number of charge carriers obtainable from a single photon. Presently, the essential objective is to rationalize the fundamental mechanisms of singlet fission, with the aim of pinpointing the microscopic characteristics of the chromophores that would be optimal for this purpose. The studies in this direction are still underway.

The processes that have to be studied are rapid, so they require fast techniques of investigation. A popular one is femtosecond pump−probe spectroscopy (FPPS), where the pumping step, effected by a femtosecond coherent light pulse (10−20 fs), promotes the chromophore from its ground state (S_0) to the first excited singlet state (S_1), concurrently generating nonstationary vibrational wave packets.[10,11]

By internal conversion, the excited singlet relaxes radiationlessly to the zero-spin component of the entangled triplet pair (T_1T_1), typically with phase coherence of the vibrational wave packet also being conserved. For pentacene derivatives, this relaxation step takes about 100 fs. After the delay of up to 1000 fs (counting from the pump pulse), the vibrational wave packets on the T_1T_1 potential energy surface (PES) are examined by the probing pulse (e.g., in ref 10 this was of 300 fs duration).

Probe absorption is recorded in the range of the $T_2 \leftarrow T_1$ or $T_3 \leftarrow T_1$ band, depending on the specific compound and researchers' priorities. It is modulated by oscillatory contributions due to the above-mentioned vibrational wave packets in the initial T_1 state. At each probe wavelength the spectrum is resolved by fast Fourier transform (FFT) into the frequencies of the normal modes forming the packets. The final results are the squared moduli of the transform coefficients ($|FFT|^2$), integrated over all the $T_n \leftarrow T_1$ absorption band in hand. This is the coherence power spectrum to be interpreted.

Except for the probing step, but including the radiationless conversion stage(s), such an experiment resembles triplet state generation (after the initial photon absorption) in an optoelectronic device; this establishes a direct link, however long, between such experiments and technological applications.

Received: July 16, 2020
Revised: September 21, 2020
Published: October 19, 2020

https://dx.doi.org/10.1021/acs.jpcc.0c06504
J. Phys. Chem. C 2020, 124, 23501−23510

In our recent papers[12,13] we have focused on the vibrational coherences generated in the pumping step of an FPPS experiment and later propagating on the singlet and triplet-pair potential energy surfaces. We have mentioned the hypothetical coherences spontaneously developed during the fission process[11] only insofar as we could, based on the overall vibrational coherence balance, draw conclusions concerning the size of their putative contribution to experimental spectra. Here we intend to continue the same strategy.

No matter how a coherent wave packet in a given vibrational mode is induced in the transition between different electronic states, the resultant periodic oscillations in time are governed by the displacement in space between the vibrational equilibrium positions of the pertinent states, which is referred to as the Franck−Condon (FC) parameter [its halved square, the Huang−Rhys (HR) factor, is used alternatively]. Technically, these parameters are the input that indispensably underlies the subsequent theoretical reconstitution (by means of a separate numerical procedure) of the vibrational coherence spectra measurable in femtosecond pump−probe spectroscopy. Quantum chemical evaluation of FC parameters is pretty straightforward for singlets, but it is less willingly undertaken for transitions within the triplet electronic manifold.[6] For this reason, the parameters for triplets are (explicitly or implicitly) adopted from the singlet results.

This assumed relationship, which implicitly underlies the fits of Bakulin et al.[14] and is picked up by other authors,[6,15] is not always apt. As we are going to demonstrate in the present paper, the differences are not necessarily large in size, but some of them affect the FPPS spectra at their most vulnerable points,[12,13] that is, at the interpretationally vital spectral features, the misreading of which might tip the qualitative physical conclusions in either of opposite directions.

An example of how precise evaluation of FC parameters can affect the interpretation of FPPS spectra was encountered recently while addressing the (pivotal) issue of determining whether or not creation of coherent vibrational wave packets (CVWP) is a vital element of the fission process itself. Originally, the pioneering experiment of Musser et al.[10] on bis-triisopropyl-silylethynylpentacene (TIPS-pentacene) led to the conclusion that in the fission process the (pump-generated) CVWPs in a number of vibrational modes were smoothly transferred from the singlet to the triplet manifold. Subsequently, a related experiment on bis-triisopropyl-silylethynyltetracene (TIPS-tetracene)[11] inspired the conjecture that coherent wave packets in one of the observed modes were *generated by SF itself*. This opened the question of whether the same could have occurred in the original TIPS-pentacene study of Musser et al. To solve this problem, the coherence balance made in theoretical calculations[12] revealed that all coherent packets observed in the probing step of that experiment were plausibly accounted for by the pumping step, and there was no leeway for additional ones to be postulated as interposed by the radiationless transition (fission). Although this finding did not preclude formation of coherent vibrational wave packets in individual SF cases, it refuted the hypothesis of their formation being a constitutive feature of singlet fission in general.

Subsequently, a similar line of research[13] demonstrated the FPPS coherence spectra to be very sensitive to the identity of a specific compound, exposing the need for caution in using superficial features of chemical likeness as foundation to appoint one molecule as a model of another for interpretational purposes. As will be shown below, this kind of circumspect attitude must also be exercised when dealing with FC parameters for singlet and triplet manifolds.

On the basis of our earlier papers where the FPPS spectra were calculated for TIPS-pentacene[12] (yielding very good agreement with experiment)[10] and pentacene[13] (alerting us to the pitfalls of chemical similitude in FPPS vibrational coherence spectroscopy), we have accumulated some experience in this kind of computations, worked out the tools to analyze coherent wave packets, and collected numerical values of the parameters that will be directly usable here. Hence, these two molecules will now serve as our model cases.

2. METHODS

The theoretical model of femtosecond pump probe spectroscopic (FPPS) investigation of singlet exciton fission used in this paper refers to the three-pulse experiment reported in ref 10 where the (weak) signal due to ground state coherences is separated out and eliminated from the triplet−triplet transient absorption spectra by a combination of experimental procedure and numerical processing. Accordingly, only the coherences resulting from genuine triplet−triplet excitations contribute to the net power spectrum and are taken into account herein. As mentioned in the Introduction, this spectrum consists of the squared moduli of the FFT coefficients ($|\mathrm{FFT}|^2$), integrated over all the $T_n \leftarrow T_1$ absorption band in hand. Its theoretical reproduction is the target of our calculations.

Our model describes a pair of identical molecules (a dimer) and is rooted in the diabatic description of that phenomenon. In a nutshell, the experiment outlined above is viewed herein as a sequence of the following steps:

(1) Pumping: induced by a femtosecond laser pulse optical transition from a moiety's stationary ground (electronic and vibrational) state to an electronically excited singlet state with a nonstationary vibrational wave packet propagating on this state's potential energy surface (PES).

(2) Fission: spontaneous triplet exciton transfer from the originally singlet-excited molecule (which is then left in its lowest triplet state, and retains the vibrational wave packet in an unaltered form) to its neighbor, whereby a (spin zero) entangled pair of triplet excitons is formed.

(3) Probing: induced by a long probe pulse optical transition from the vibrational wave packet propagating on the T_1 triplet PES of the originally singlet-excited molecule to a stationary vibrational state on the T_n PES.

As mentioned in the Introduction, the measurements are performed in a time-dependent regime, with an adjustable offset between the short pump pulse and a much longer probe pulse (broad-band white light continuum). Absorption of the latter (to be theoretically reproduced) is recorded in temporal and spectral resolution.

The precise mechanism of the fission process itself (i.e., the radiationless transition between the S_1 and T_1T_1 states of the dimer) is out of our present scope. It does not seem to directly influence the final shape of the registered coherence spectra,[10] and for this reason there is no need to consider it explicitly herein. Hence, in the second step above it is viewed as a black box, of which the second (triplet recipient) molecule is a part, so ultimately a projection of all the process onto the subspace of the first (initially excited) molecule is monitored.

Ultimately, once the conditions of the experiment (such as temporal resolution and the duration of the pumping and

https://dx.doi.org/10.1021/acs.jpcc.0c06504
J. Phys. Chem. C 2020, 124, 23501−23510

probing pulses) are defined, the Fourier transformation directly yields the sought power spectrum of coherent vibrational wave packets. The necessary formulas are accessible in Supporting Information sections 1−5. To inspect their derivation and wider commentaries, the reader is referred to our earlier papers[12,13] and their Supporting Information.

Being implicitly rooted in the diabatic picture, the model outlined above reduces the description of the pumping step to calculations of the FC integrals between the chromophore ground (S_0) and lowest excited singlet state (S_1). Likewise, the description of the probing step is reduced to the calculations of analogous integrals between the directly involved $T_1 = 1^3B_{2u}$, $T_2 = 1^3B_{1g}$, and/or $T_3 = 2^3B_{1g}$ triplet states.

It should be mentioned in passing that the labeling convention for the pertinent states that is accepted in the field[10] is based on the D_{2h} symmetry group of the pentacene molecule and takes into account only the states that are dipole-allowed from T_1 (the transition energies being about 1.70 and 2.21 eV for T_2 and T_3, respectively). In reality, two more triplet states[14] (2^3B_{2u} and 1^3B_{3u}) are bracketed between T_2 and T_3, but the corresponding transitions from T_1 are forbidden by symmetry.[16] Effectively, in general count T_3 is the fifth triplet state of the molecule.

The final pattern of relative coherence intensities of different modes is expressed in terms of the products of FC integrals relevant for the pumping and for the probing step (cf. Supporting Information, Sections 1−5). The requisite FC parameters are computed using generally accessible quantum chemistry programs. In our earlier work[17] we tested the performance of the CC2 approach (with various basis sets) and of the DFT methodology with different energy functionals (and basis sets) in calculating vibronic relaxation energies for a large group of molecules. The results revealed that for systems of pentacene size the B3LYP energy functional with def2-TZVPP basis affords the best description. The comparison with CC2 was repeated specifically in the TIPS-pentacene context and corroborated this choice. Consequently, it is presently our routine to calculate the requisite FC parameters by using the TURBOMOLE V6.4 2011 collection of quantum chemistry programs,[18] specifically the TDDFT module thereof, with B3LYP energy functional and def2-TZVPP basis. The T_1 state is then viewed as the ground state in the triplet manifold, whereas the higher triplet states are generated by the TDDFT scheme. The geometries of the states of interest are subsequently optimized (they are readily available in the Supporting Information, section 7), and the normal modes are calculated. The FC parameters are then obtained by appropriate projections of the geometry changes between the different electronic states of interest (cf. Figure 1a).

All the input data needed to calculate the CVWP spectra for TIPS-pentacene and pentacene (which will be our examples herein) are listed in refs 12 and 13. Accordingly, in the following all input is exactly the same as that in our earlier papers, with the exception of the FC parameters.

In this latter regard, our present calculations will be split into two parallel approaches differing in the adopted values of the FC parameters for the triplet manifold. In the first one, to be hereafter referred to as "complete model", we will use the FC parameters originally calculated for the specific triplet−triplet transitions addressed (as was done in our earlier papers).[12,13] In our second approach, to be called "truncated model", for the transitions in the triplet manifold the $S_1 \leftarrow S_0$ FC parameters will be consistently used, as if the calculations for the triplet manifold have never been performed; this will simulate the practice commonly adopted in the literature.[6,14,15]

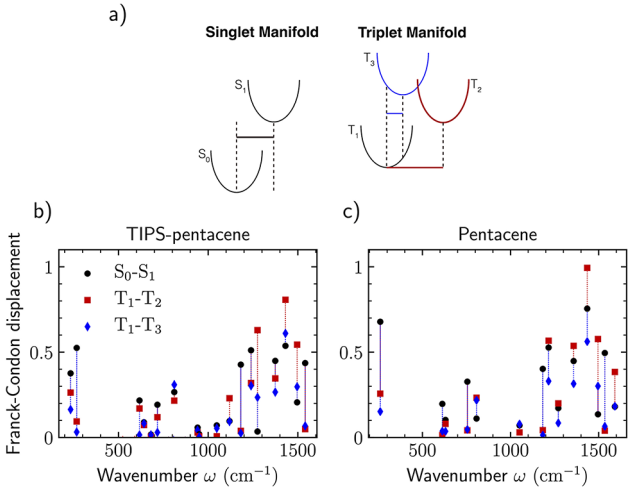

Figure 1. FC parameters (used in the complete model) as a function of vibrational frequency for the $T_2 \leftarrow T_1$ (red squares) and $T_3 \leftarrow T_1$ (blue diamonds) transitions, compared to those that replace them in the truncated model and are borrowed from the singlet manifold ($S_1 \leftarrow S_0$). (a) Parameter visualization, (b) TIPS-pentacene, and (c) pentacene.

For the example systems we will now be investigating, namely, TIPS-pentacene and pentacene, these FC parameters are summarized in Figure 1b,c, respectively. Each figure encompasses all normal modes that exhibit non-negligible displacements of equilibrium positions upon the corresponding electronic transitions.

The black dots represent the FC parameters for the singlet transition ($S_1 \leftarrow S_0$) that are used in the second approach, replacing those calculated specifically for the $T_2 \leftarrow T_1$ and $T_3 \leftarrow T_1$ transitions used in the first approach (red squares and blue diamonds, respectively). They give an idea of the parameter changes introduced by the truncated model, to be related to the resultant changes in the spectra that are to be presented further on.

3. RESULTS AND DISCUSSION

3.1. Example: TIPS-Pentacene. The experimental CVWP spectra of TIPS-pentacene, probed in the $T_2 \leftarrow T_1$ and $T_3 \leftarrow T_1$ wavelength ranges, are displayed in Figure 2a,b, respectively, along with their theoretically reproduced counterparts (with all FC parameters calculated individually for each pair of electronic states engaged in the indicated transition, as described above). To reduce the computational effort, those calculations were actually performed for the model molecule of 6,13-bissilylethynylpentacene (SE-pentacene), which in view of the spectral insignificance of the differences is consistently viewed as equivalent.

Account taken of the limited intrinsic experimental accuracy (especially in view of the high background noise in the weak $T_2 \leftarrow T_1$ transition), and all inherent errors of the complex data collection and numerical processing procedures, combined with the limitations of the highly idealized theoretical model, the agreement with experiment may be considered remarkably good. To forestall putative confusion about the good agreement, it should be stated at once that the apparent peak at 1150 cm^{-1} is in reality an artifact of the procedure applied in ref 10 to eliminate (by using a combination of a

https://dx.doi.org/10.1021/acs.jpcc.0c06504
J. Phys. Chem. C 2020, 124, 23501−23510

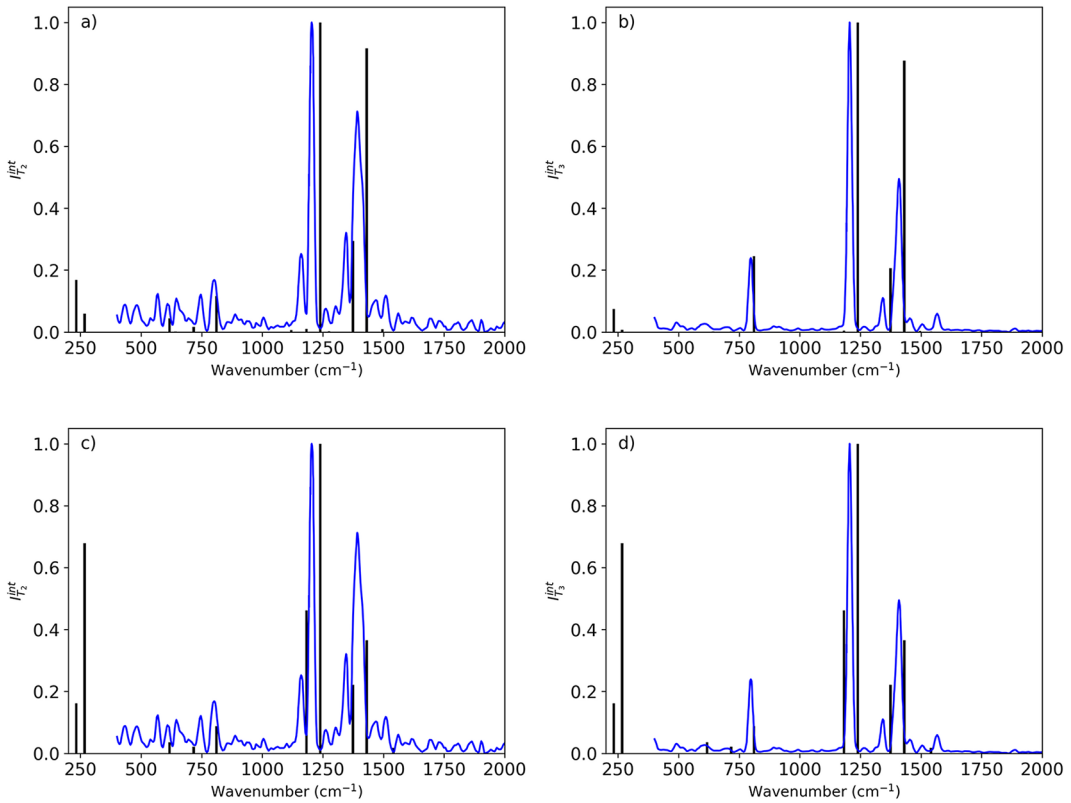

Figure 2. Calculated coherence power spectrum of TIPS-pentacene (sticks) compared with the experimental vibrational coherence spectrum (continuous line, from ref 10). Complete model: (a) $T_2 \leftarrow T_1$, (b) $T_3 \leftarrow T_1$ transition. Truncated model: (c) $T_2 \leftarrow T_1$, (d) $T_3 \leftarrow T_1$ transition.

dump pulse and numerical processing) the spurious signals due to S_0-originating coherences. The consistently overrated vibrational frequencies are an inevitable consequence of employing the B3LYP functional and neglecting anharmonicities. The intensities around 1400 cm^{-1} seem somewhat overestimated, especially for the $T_3 \leftarrow T_1$ transition. This is, however, only apparent, being caused by the stick representation of the power peaks (which takes no account of the large experimental width of that band). The details on these issues are to be found in ref 12.

Prior to further discussion, it seems recommendable to expose the interpretational role of the individual features in the calculated spectra. The leading spectral peaks at 1239, 1374, and 1431 cm^{-1} (with the frequencies and the relative contributions reproduced as expected of the applied methodology) are documenting the ability of our approach to correctly build the interpretational framework of the CVWP system under study, serving as a sort of an internal standard.

On the other hand, the peak at around 800 cm^{-1} is of paramount interpretational importance providing a response to the literature hypothesis[11] that in addition to a pair of triplet excitons singlet fission creates a coherent vibrational wave packet. The wave packet to which this provenance was attributed had been presumably detected for TIPS-tetracene[11] just at the frequency of 760 cm^{-1} (i.e., in the vicinity of the pertinent TIPS-pentacene mode). The entire coherence power spectrum of this latter system was plausibly reproduced by our calculations (cf. Figure 2a,b), and specifically for the 811 cm^{-1} mode, the rendering is practically perfect in both triplet−triplet transitions under investigation. This was achieved without invoking any coherence source other than the pump, and comparison of our results with the experimental spectrum[10] leaves no room for any additional coherence contribution. This demonstrates that at least in TIPS-pentacene creation of a coherent wave packet does not occur; hence, it is not necessary for effective fission, which proves that it is not an indispensable element of the singlet fission mechanism in general.

Finally, the two additional very weak bands (617 and 717 cm^{-1}), presumably present in the $T_2 \leftarrow T_1$, but absent (or negligibly weak) in the $T_3 \leftarrow T_1$ spectrum, might be another factor further corroborating the reliability of the applied approach, lending it yet more credence. This is admittedly somewhat tenuous, since (because of the low $T_2 \leftarrow T_1$ transition intensity) they are observed merely as two more wiggles in a noisy spectral region (Figure 2a), but their absence in the (practically noise-free) $T_3 \leftarrow T_1$ range (Figure 2b) is at least consistent with the overall picture. The low-frequency signals around 250 cm^{-1} are located beyond the experimental range, so they can neither support nor refute the validity of the approach, and will be discussed jointly with the corresponding mode of pentacene (vide infra).

Figure 2c,d depicts the same $T_2 \leftarrow T_1$ and $T_3 \leftarrow T_1$ coherence spectra, but they are simulated with the $S_1 \leftarrow S_0$ FC parameters used instead of those calculated for the triplet manifold, all other things being equal (truncated model). The new simulations exhibit the following striking features: (1) In both wavelength ranges, a prominent peak appears at 1182 cm^{-1}. It has no counterpart in either experimental spectrum; misleadingly, in the noisy $T_2 \leftarrow T_1$ case (cf. Figure 2c) it is located quite close to the artifact band at 1150 cm^{-1}. (2) In both wavelength ranges, the intensity of the second-largest 1431 cm^{-1} peak is strikingly reduced, which makes it evidently underestimated. (3) The intensity of the interpretationally critical 811 cm^{-1} peak is also reduced in both wavelength

https://dx.doi.org/10.1021/acs.jpcc.0c06504
J. Phys. Chem. C 2020, 124, 23501−23510

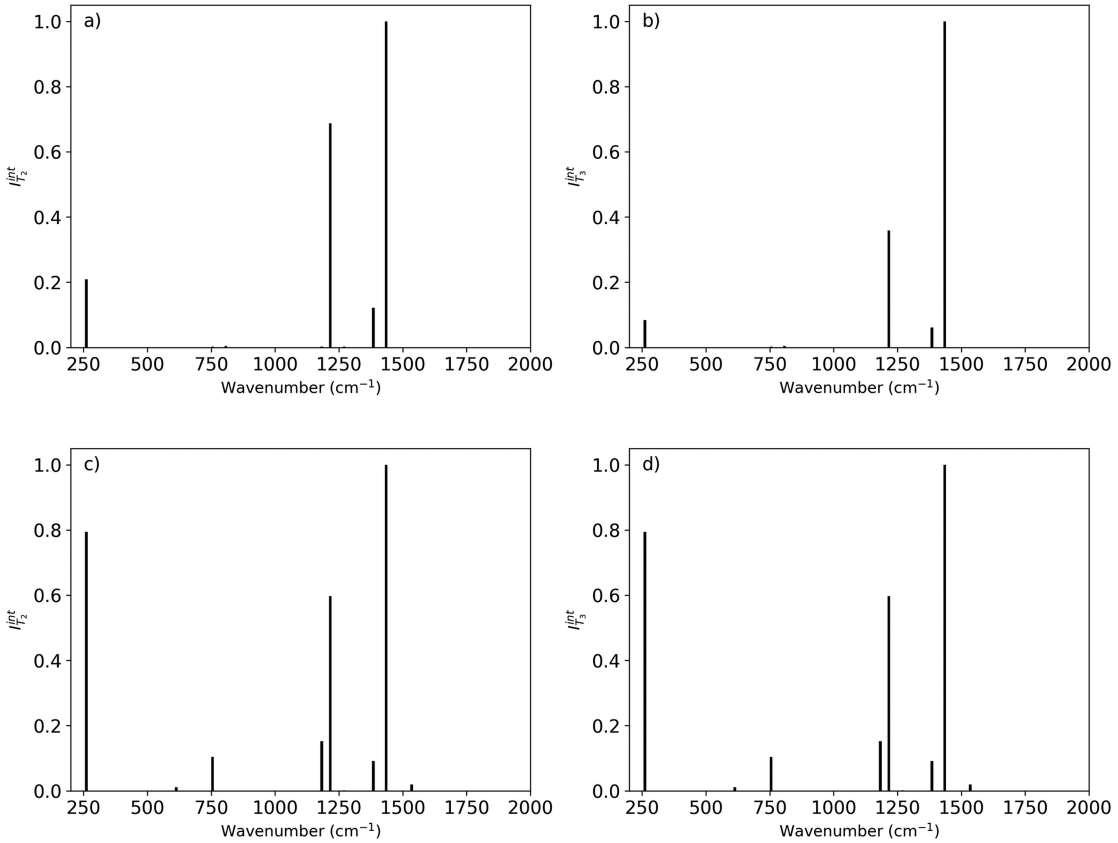

Figure 3. Calculated coherence power spectrum of pentacene. Complete model: (a) $T_2 \leftarrow T_1$, (b) $T_3 \leftarrow T_1$ transition. Truncated model: (c) $T_2 \leftarrow T_1$, (d) $T_3 \leftarrow T_1$ transition.

ranges, perceptibly for $T_2 \leftarrow T_1$ (Figure 2c vs 2a) and substantially (almost 3-fold) for $T_3 \leftarrow T_1$ (Figure 2d vs 2b). (4) In contrast, the 267 cm^{-1} signal acquires enormous power.

It should first be noted that the overall agreement with the measured spectra is now much poorer. Next, we will explore the putative interpretative consequences.

3.2. Gedanken Experiment. As a "gedanken" (thought) experiment, let us presently suppose that in our original calculations of ref 12 the truncated model was adopted, with the FC parameters for triplet−triplet transitions borrowed from the results obtained for the singlet manifold, the results of the complete model being unknown. Then the conclusions concerning putative coherence generation in singlet fission would dramatically change.

In that case, our reasoning would have been based on Figure 2c,2d. The 1431 cm^{-1} peak would then be evidently underrated but close enough to its measured intensity to declare its rendering more or less acceptable (possibly suggesting some coherence generation in this mode caused by the fission process).

This issue calls for an extra comment. A band intensity predicted to be lower than actually observed might have two reasons: either inherent discrepancy of the computational method or the coherence surplus generated by fission, which by assumption is not included in our model (truncated and complete alike). As there is presently no alternative method of translocating a vibrational wave packet from the S_1 to the T_1T_1 PES, the fission event on the way cannot be avoided. Hence, for the time being there are no means to extract either of the two possible contributions separately. As coherence necessitates rather special conditions to emerge, it is not expected to be very common, and an inherent deficiency of a quantum chemistry method is a more likely explanation. In our original calculation (complete model),[12] no such ambiguity ensued because the calculations exhibited no coherence deficit with respect to experiment. In the truncated model described here, this ambiguity does exist (vide infra).

The 1182 cm^{-1} peak, however (spurious, as we know, and only seemingly identifiable with an artifact in the weak $T_2 \leftarrow T_1$ spectrum of Figure 2a), presents just a reverse difficulty. According to the truncated model, it is predicted to be prominent in both transitions under scrutiny, in blatant disagreement with experimental findings. With our present hindsight based on the complete model results,[12] we view this as a conclusive argument to reject the simplistic singlet-copying approach (truncated model). However, if these latter calculations were performed first, as we now hypothetically assume, then there would have been no benchmark data to appeal to, yet to rationalize the disagreement with experiment, the divergence could readily be blamed on scattering-induced phase and/or amplitude relaxation at any point of packet propagation.

Continuing now the overview of (truncated model) vibrational modes, the evident intensity deficit in the 811 cm^{-1} vibration would have been a reasonable argument in favor of coherence generation in this mode at the fission stage. For both wavelength ranges, it would imply that in addition to the coherence supply provided at the pumping stage, there was also another contribution, from 1/2 (Figure 2c) to 2/3(Figure 2d) of the observed total. In effect, if we had used in our calculations[12] the singlet FC parameters for triplet−triplet transitions, then we would have reached the conclusion that

https://dx.doi.org/10.1021/acs.jpcc.0c06504
J. Phys. Chem. C 2020, 124, 23501−23510

vibrational coherence is indeed generated in singlet fission, as originally proposed by Stern et al. for TIPS-tetracene. This conclusion would have been contrary to the one we did actually reach using the proper triplet FC parameters, and which we consider correct. The above inference demonstrates the critical interpretational importance the proper values of the FC parameters have in vibrational coherence spectroscopy. Although for most vibrations the discrepancies between the parameters obtained from the truncated and the complete model are substantial, they may still be of marginal consequence. Paradoxically, it might be just the tiny differences in some crucial modes that could tip the balance between the correct and an incorrect view of the phenomenon under study.

3.3. Pentacene: Spectral (Dis)Similarities. We have recently demonstrated with theoretical calculations[13] that in the context of femtosecond pump−probe spectroscopy of coherent vibrational wave packets the spectral differences between TIPS-pentacene and pentacene preclude treating these two systems as two different incarnations of the same generic chromophore (cf. Figures 2a,b and 3a,b), in contrast to the situation in more traditional spectroscopic domains where this concept is successfully employed. However, it sometimes happens that subtleties of this kind disappear when less sophisticated theoretical approaches are used. We presently test whether this is the case in the truncated model where the FC integrals for transitions in the triplet manifold are assumed to be the copies of their singlet counterparts. Comparison of Figures 2c,d and 3c,d shows that this does not happen here: The substantial difference between the TIPS-pentacene and pentacene spectra remains valid also when they are calculated within the truncated approach. This precludes application of the TIPS-pentacene experimental spectrum as reference for pentacene (or vice versa) also at the less rigorous truncated-model level of theory.

It should be noted that truncation of the model alters the predicted pentacene spectra (cf. Figure 3c,d vs 3a,b) somewhat differently from those of TIPS-pent (cf. Figure 2c,d vs 2a,b). The spurious 1183 cm^{-1} peak does appear also in pentacene, just as it did in its derivative compound, but with a drastically reduced intensity. The 807 cm^{-1} signal (absent in the complete model, Figure 3a and 3b) remains mute, but a new coherence now appears at the modified frequency of 755 cm^{-1}, contrary to the situation in TIPS-pentacene where model truncation, in contrast, diminished the intensity of the 811 cm^{-1} vibration (the change, although only slight, is interpretationally crucial; vide supra). Also, in contrast to the situation in TIPS-pentacene where upon model truncation the relative intensity of the 1239 cm^{-1} peak with respect to that at 1431 cm^{-1} grows in both spectral ranges under study, for pentacene it diminishes for the $T_2 \leftarrow T_1$ range (Figure 3c), although it does increase for $T_3 \leftarrow T_1$ (Figure 3d).

Probably the only indubitable similarity can be found in the skyrocketing contribution of the mode around 260 cm^{-1}. Overall, any comparative cross-referencing targeted at seeking consistent analogies of coherence behavior between these two compounds seems to be a failure. Despite their chemical likeness, in this specific regard they turn out to be quite different.

3.4. Coherence Flow. Our present task is to analyze the mechanism of changes in the coherence relative intensities upon altering the model used for their simulations from the complete to the truncated one. To this end, we employ the concepts introduced in our recent papers[12,13] to which the reader is referred for details.

The final formula [eqs S2 and S3], derived in ref 12 and used to generate the spectra presented above, describes the rate of probe-induced $T_n \leftarrow T_1$ transition from the coherent vibrational wave packet generated in the T_1 state by the radiationless transition from the S_1 state in which the vibrational coherence was initiated by the pumping pulse. In the said formula the parts relating to the pumping and probing steps of the experiment are coupled in a way that is inconvenient for dealing with the singlet (pump) and triplet (probe) manifolds separately. Our present point is to analyze the consequences of the change that affects the triplet subspace alone (replacing the triplet FC parameters by the singlet ones). This is facilitated by invoking approximate descriptors that separately address:

(1) Wave packet supply by pumping in the singlet manifold:

$$J_{S_1}(\omega_\chi) = \sum_{j=0}^{\infty} c_j c_{j+1} \tag{1}$$

where $c_j = |F_{j,0}^{S_1,S_0}| \cdot \sqrt{G(\omega_{S_1} + j\omega_\chi)}$ is the weight of the jth vibrational stationary state in the nonstationary wave packet generated in the mode ω_χ by the pump with spectral profile $G(E)$. $\omega_{S_1} = \varepsilon_{S_{11}}/\hbar$ stands for the S_1 excitation energy expressed in frequency units. The symbol F_{ij}^{PR} denotes the FC integral between the ith vibrational eigenstate in the Pth electronic state and the jth vibrational eigenstate in the Rth electronic state.

2. Triplet coherence detection factor:

$$J_{T_n}(\omega_\chi) = \left| \sum_{i=0}^{\infty} F_{0,i}^{T_n,T_1} F_{0,i+1}^{T_n,T_1} \right| \tag{2}$$

The final result ($|FFT|^2$) is also proportional to the damping factor η resulting from the finite temporal resolution of the experimental equipment [cf. eqs S4 and S5]. Its main role consists in reducing the intensities of high frequency modes,[10,12−14] and will not be discussed here, as it is irrelevant in the present context.

The quantities of current interpretational importance are collected mode by mode (identified by frequency ω_χ) in Tables 1 and 2 (for TIPS-pentacene and pentacene, respectively). Each table includes all modes of the molecule in hand that are endowed with non-negligible pertinent Franck-Condon parameters. $J_{S_1}(\omega_\chi)$ are the coherence supply factors (vide supra) determined (apart from the FC parameters) also by the characteristics of the pumping laser. $J_{T_n}(\omega_\chi)$, defined by products of the FC integrals, stand for the triplet coherence detection factors (detectabilities), and do not depend on the conditions of the experiment. They account for the molecule's propensity to transform the coherent vibrational oscillations on the T_1 potential energy surface into the modulation of $T_n \leftarrow T_1$ absorption which is ultimately registered. The product $J_{S_1}J_{T_n} = J_{S_1}(\omega_\chi)\, J_{T_n}(\omega_\chi)$ of the two descriptors provides an approximate measure of the pertinent coherence power.

The counterparts of the J_{T_n} values, obtained within the truncated model where the *triplet* FC parameters are replaced by the corresponding *singlet* ones, will be denoted by J_{ST}. They are [by definition of eq 2] the same for both triplet−triplet

https://dx.doi.org/10.1021/acs.jpcc.0c06504
J. Phys. Chem. C 2020, 124, 23501−23510

Table 1. Descriptors of Coherence Flow Calculated for TIPS-pentacene

ω, cm^{-1}	J_S[a]	J_{T_2}	J_{ST}	J_{T_3}	$J_S J_{T_2}$	$J_S J_{ST}$	$J_S J_{T_3}$
233	0.009	0.184	0.260	0.116	0.002	0.002	0.001
267	0.016	0.066	0.357	0.023	0.001	0.006	0.000
617	0.016	0.120	0.152	0.011	0.002	0.002	0.000
642	0.005	0.052	0.063	0.058	0.000	0.000	0.000
717	0.018	0.084	0.135	0.021	0.002	0.002	0.000
811	0.045	0.152	0.186	0.215	0.007	0.008	0.010
941	0.006	0.021	0.041	0.030	0.000	0.000	0.000
950	0.001	0.005	0.013	0.002	0.000	0.000	0.000
1048	0.010	0.005	0.050	0.038	0.000	0.000	0.000
1119	0.016	0.161	0.068	0.066	0.003	0.001	0.001
1182	0.501	0.028	0.294	0.018	0.014	0.147	0.009
1239	1.000	0.222	0.348	0.211	0.222	0.348	0.211
1275	0.006	0.420	0.025	0.165	0.002	0.000	0.001
1431	1.717	0.521	0.364	0.409	0.894	0.625	0.702
1374	0.894	0.240	0.308	0.186	0.215	0.276	0.166
1496	0.136	0.369	0.145	0.207	0.050	0.020	0.028
1541	1.107	0.035	0.300	0.048	0.038	0.332	0.053
1598	0.135	0.264	0.135	0.166	0.036	0.018	0.022

[a]Arbitrary units.

Table 2. Descriptors of Coherence Flow Calculated for Pentacene

ω, cm^{-1}	J_S[a]	J_{T_2}	J_{ST}	J_{T_3}	$J_S J_{T_2}$	$J_S J_{ST}$	$J_S J_{T_3}$
261	0.024	0.180	0.449	0.107	0.004	0.011	0.003
613	0.013	0.010	0.139	0.026	0.000	0.002	0.000
631	0.006	0.057	0.073	0.025	0.000	0.000	0.000
755	0.056	0.030	0.228	0.033	0.002	0.013	0.002
807	0.010	0.163	0.078	0.153	0.002	0.001	0.002
1051	0.009	0.021	0.050	0.056	0.000	0.000	0.001
1183	0.401	0.030	0.278	0.010	0.012	0.111	0.004
1216	1.000	0.383	0.358	0.230	0.383	0.358	0.230
1271	0.058	0.141	0.121	0.060	0.008	0.007	0.003
1435	4.493	0.614	0.493	0.380	2.758	2.214	1.707
1385	0.805	0.364	0.308	0.220	0.293	0.248	0.177
1496	0.052	0.389	0.096	0.210	0.020	0.005	0.011
1535	1.457	0.028	0.338	0.046	0.041	0.492	0.067
1592	0.111	0.266	0.127	0.129	0.030	0.014	0.014

[a]Arbitrary units

transitions; hence, only one J_{ST} and one $J_S J_{ST}$ column are presented in the table and for easier comparison are placed between the columns corresponding to the two triplet states.

The last three columns of both tables demonstrate how only a few of the totally symmetric vibrations are really likely to yield in femtosecond pump−probe spectroscopy a non-negligible coherently modulated signal.

In TIPS-pentacene, the first truly noticeable signal in the actually scanned observation range appears at 811 cm^{-1} (columns 6 and 8). Its size results from the coincidence of medium-sized pump-generated coherence supply (column 2) and relatively high triplet detectability (columns 3 and 5). The FC parameters for triplets (embodied in the detectabilities of columns 3 and 5) are comparable in size to those in the singlet manifold (column 4), so truncation of the model only slightly changes the coherence power (cf. column 7 vs 6 and 8).

In contrast, the high coherence supply (due to large singlet FC parameters) makes the truncated model favor the 1182 cm^{-1} mode. The same mechanism strengthens the predominance of the 1239 cm^{-1} vibration, increasing its preponderance over the 1431 cm^{-1} mode. Although the latter (as also evidenced by its impressive coherence supply) is endowed with large singlet FC parameters, its FC parameters in the triplet manifold are evidently still larger, such that their replacement in model truncation diminishes the net result. On the contrary, the nearby 1374 cm^{-1} mode, with triplet FC parameters smaller than that for the singlet (cf. Figure 1b), resembles in its behavior the lower frequency vibrations described earlier (vide supra). At first glance, this might be expected to cause amplification of its signals upon model truncation, but that effect is compensated by the concurrent increase in the absolute intensity of the 1239 cm^{-1} vibration (as mentioned above) that is used as reference for the relative intensities. The net effect is a truncation-induced minor enhancement of the 1374 cm^{-1} signal in the $T_2 \leftarrow T_1$ transition (cf. Figure 2c vs 2a) and its barely discernible reduction in the $T_3 \leftarrow T_1$ one (cf. Figure 2d vs 2b).

The above is to be compared with pentacene (cf. Figure 1c), where the trend in the relation between the 1385 and 1435 cm^{-1} modes is reversed, since the latter's enormous coherence supply becomes the leading feature, so this peak even supersedes the contribution from the 1216 cm^{-1} vibration (dominant for TIPS-pentacene). The intruder at 1183 cm^{-1}, originally practically mute (columns 6 and 8) because of low triplet detectability (columns 3 and 5), gains importance upon model truncation (column 7), owing to the large singlet FC parameters that replace the triplet ones (columns 3 and 5). This resembles the situation in TIPS-pentacene.

The power of the 807 cm^{-1} mode is negligible here, largely because of the low initial supply (lower than in TIPS-pent), and is barely affected by switching to the truncated approach (since, like in TIPS-pentacene, the singlet FC parameters of this vibration are smaller than the triplet ones). As follows from our earlier discussion in ref 13, the absence of TIPS substituents substantially affects the intermode coupling by restoring a large share of the central-ring molecular displacements to the 755 cm^{-1} mode, thereby increasing its singlet FC parameters. This change evidently suffices to provide in the truncated model a J_{ST} value considerably larger than the genuine triplet parameters.

Having no direct experimental data concerning the low-frequency coherences around 260 cm^{-1}, we now discuss them separately. As mentioned above, the behavior of this mode is similar in both compounds under study, which is not surprising since this vibration stretches the pentacene molecule along its long axis, only marginally engaging the outer (6, 13) carbon atoms of the central ring, and leaving the TIPS substituents perfectly intact. In pentacene, the 261 cm^{-1} vibration represents an intermediate case, with medium-low singlet supply and medium triplet detectability. In the complete model it gives an appreciable contribution, which owing to the unusually high singlet FC value exhibits spectacular increase in the truncated model. In TIPS-pentacene, the effect of the added massive groups is not entirely negligible; they do constrain the motion of the said carbon atoms to some extent. As a consequence, the FC parameters for the 267 cm^{-1} mode are reduced, diminishing singlet supply and triplet detectability, with the same effect on the coherence intensities. Also in this compound, however, the detectability descriptor for the

https://dx.doi.org/10.1021/acs.jpcc.0c06504
J. Phys. Chem. C 2020, 124, 23501−23510

singlet transition is substantially larger than for triplets, leading to an enormous power increase upon model truncation.

In contrast, the 233 cm^{-1} mode of TIPS-pentacene engages primarily the substituents [and to some extent the (6, 13) carbon atoms, to which the substituents are bonded], so it has no direct counterpart in pristine pentacene. The large mass of TIPS groups explains the relatively low frequency of this vibration. Their participation completely disrupts some normal coordinates of the pentacene core, especially that at 763 cm^{-1}, which is no longer discernible in the TIPS-pentacene spectrum. In pristine pentacene, this parent mode is an in-phase stretch of all rings along the short molecular axis, and upon (6, 13) substitution it congruously combines with the in-phase motion of the TIPS groups along that direction. This coupling distinguishes the central ring from the others, eliminating contributions of the latter from the resultant 233 cm^{-1} mode. Such a trend, by the way, concurs with purely electronic effects: The optimum geometries in all the electronic states under study have the central ring elongated (to a varying extent) in the direction of the short molecular axis. Ultimately, in all electronic transitions the vibronic activity of the 233 cm^{-1} vibration is mostly determined by geometry changes within the central pentacene ring, with negligible contributions from other regions of the molecule. This fundamentally changes the balance in the FC parameters, which for the parent 763 cm^{-1} modes are dramatically suppressed by mutual cancellation of the contributions from the central, adjacent, and terminal benzene rings. With the above view, the relatively large values of these parameters for the 233 cm^{-1} mode in TIPS-pentacene triplet−triplet transitions are an inevitable consequence.

Summarizing, in contradistinction to the 267 cm^{-1} mode, the 233 cm^{-1} vibration is endowed with considerable FC parameters, on the order of the singlet ones, so the model truncation affects its coherence power and coherence flow only slightly.

Even though there is no direct experimental confirmation, we deem the above rationalization of the reported results concerning the low-frequency modes sufficient to lend credence to the consistency of the overall physical picture we are proposing. We do hope, however, that future experimental effort will also corroborate the predicted intensities of the low-frequency coherences.

3.5. Soft Selection Rules. In an electronic optical transition, a vibrational wave packet is generated by synchronous coherent excitation of at least two vibrational eigenstates. To this end, the spectral profile of the pumping pulse must energetically encompass both of them. This is set by the conditions of the experiment and can be read out from column 2 of the above tables (more details are available in refs 12 and 13).

Both of these eigenstates must exhibit nonzero overlap with the initial state vibrational wave function, which implies a nonzero shift of the vibrational equilibrium position between the engaged electronic states (i.e., a nonvanishing FC parameter). As indicated previously,[12] this may be viewed as a kind of selection rule for the pumping $S_1 \leftarrow S_0$ step of an FPPS experiment. An analogous condition must be fulfilled in the $T_n \leftarrow T_1$ step. Effectively, this is how the coherence-decisive characteristics of the molecule are engraved in its potential energy surfaces. Since the two overlap integrals enter the coherence power formula as factors in a product expression, these rules for a vibrational coherence to be induced and detected are in net effect rather demanding, since they must be satisfied in conjunction.[12] This resembles other nonlinear optical phenomena, of which pump−probe spectroscopy is in fact an example.

Individually, these selection rules are not as stringent as they seem, because an FC parameter is a continuous variable, and it depends on the context how large it must be to be deemed appreciable. Unless one of the relevant FC parameters strictly vanishes, even a considerable shortage in one factor may be compensated by a substantial value of the other (at least, no fundamental principle seems to preclude it; the TIPS-pentacene 233 cm^{-1} mode may serve as an example). In this sense, we call these selection rules "soft".

As discussed in the preceding section, the most prominent peaks in the power spectra of both molecules under study (from the frequency groups around 800, 1240, 1430, 1380, and 1540 cm^{-1}) satisfy both of the above selection rules, combining reasonably large singlet supply with substantial triplet detectability. They are also robust with respect to model change, since their singlet and triplet FC parameters are of comparable size.

In contrast, the "intruder" coherences that have surfaced upon truncation of the model (1182 and 267 cm^{-1} in TIPS-pentacene and 1183 and 755 cm^{-1} in pentacene), within the complete model may be deemed practically forbidden (nearly zero coherence flux), with consistently low characteristics in the "detectability" slot and "supply" being either downright low (267 cm^{-1}) or not sufficiently high to compensate for the former deficit (1180 cm^{-1}). (There are also some less clear intermediate cases, such as the 261 cm^{-1} vibration in pentacene.) It is to be noted in this context that each exemplary intruder mode is located in the table (vide supra) just in the immediate vicinity of a mode endowed with a considerably larger value of the triplet detectability descriptor (determined by the FC parameters). Moving one row down (or up for the 267 cm^{-1} mode), these parameters are greater by an order of magnitude.

The two modes' vicinity in the table implies their proximity in energy scale, facilitating their mixing upon any (even minor) perturbation. Actually, the change of the electronic wave function from triplet to singlet (or vice versa) is a substantial difference, with energetic effect on the order of 1 eV. On this scale, the gap of a few tens of wavenumbers between the modes that are adjacent in the flow descriptor table is negligible, so the modes may be treated as quasi-degenerate. Consequently, it is no surprise that the change from triplet to singlet is expected to induce their strong mixing, abruptly changing their individual FC parameters and in consequence the flow descriptors. Of course, this is likely to happen only to some specific mode pairs which engage the parts of the molecule that undergo major geometric rearrangements when the spin changes.

J_{ST} is formally analogous (in the sense that it is constructed in the same way) to the triplet detectability descriptors $J_{T_n}(\omega_\chi)$, with the difference that singlet FC parameters are used instead of the triplet ones. The mixing mentioned above should lead to equalization of the properties of the two vibrations being mixed. Truncation of the model, where the triplet detectability is simply replaced by its singlet analog (with no allowance for the contribution of the original mode), exaggerates the effect, especially on that member of the mode pair discussed above which was originally endowed with the smaller detectability

https://dx.doi.org/10.1021/acs.jpcc.0c06504
J. Phys. Chem. C 2020, 124, 23501−23510

value, hence the resultant disproportionate intensities of the intruder modes.

According to Figure 1, both the size and the sense of the FC parameter changes between different triplet states strikingly vary from one vibration to another. For those modes (such as 1180 cm^{-1}) along which the triplet geometry conspicuously relaxes, the pertinent FC parameters dramatically deviate from those in the singlet manifold, so model truncation is bound to enormously overrate the triplet detectabilities. By artificially forcing on the wave packet the "singlet-size" FC parameter in the triplet detectability slot, one promotes it from the "forbidden-type" to the "strongly-allowed-type" coherence regime.

3.6. Singlet FC Parameters as Triplet FC Parameter Surrogates. The main computational result of this paper is the finding that in general the singlet FC parameters are no substitute for the triplet ones. As a matter of fact, from the point of view of quantum chemistry there is no reason why they should be, yet the analysis above demonstrates that on average the truncated model where the triplet FC parameters are approximated by the singlet ones happens to be doing reasonably well. Although at a quantitative level its performance is far from perfect, in most aspects it is qualitatively acceptable. The exceptions are the "intruder" coherences described above. They evidently involve the modes that probe some unstable regions of coordinate space which are subject to substantial configurational rearrangements upon spin multiplicity change. For the time being, we have only a vague idea how to identify them, which we believe would be pretty useful for fission modeling.

Looking at the problem from a somewhat different angle, let us bear in mind that J_{ST} is formally analogous (vide supra) to the triplet detectability descriptors $J_{T_n}(\omega_\chi)$, only with the singlet FC parameters substituted instead of the triplet ones. This enables us to treat both of the adopted soft selection rules (concerning singlet "supply" and triplet "detectability") on equal footing. As shown above, the coherences that are experimentally observed are all reasonably intense and robust (with respect to model change), combining the "allowed" status in the (singlet) coherence supply and (triplet) detectability aspects. Our results suggest that generally only those are likely to attain sizable intensities; we will call these "genuine". We may adopt some arbitrary value, say 0.2, as a tentative standard of "allowedness" in each of these aspects.

Then, in an ensemble of precursor coherent wave packets generated at the truncated level, all of these must have at least about this amount in the supply slot. As stated above, for each wave packet this is just its value of J_{ST}. According to the fundamental posit of the truncated model, $J_{T_n}(\omega_\chi) \cong J_{ST}$. The contents of the "supply" and "detectability" slots are now defined for every packet; this spans the set of putative (precursor) coherences to be considered. On the basis of our present outcome, most of them are expected to be genuine (because the truncated model is usually qualitatively correct). Nonetheless, some are not, because in special cases like those pinpointed above $J_{T_n}(\omega_\chi)$ in reality substantially differs from J_{ST}, violating the fundamental proviso of the truncated model. Usually, the true $J_{T_n}(\omega_\chi)$ value (from the complete model) is smaller, so for some wave packets the actual triplet detectability will fail to attain the hypothetical threshold required to make them genuine. Thus, in these individual cases although the truncated-model (precursor) wave packet has been constructed, it is not genuine (lacking robustness to model truncation) and will not be observable.

The above inference demonstrates that the set of coherences predicted by the truncated model is likely to contain some spurious wave packets that are not physically feasible, which is probably that model's main deficiency. In fact, the coherence power spectrum generated by means of the extremely sophisticated and mostly successful Tree Tensor Network State (TTNS) algorithm[6,19] exhibits a number of peaks that have no experimental counterparts. These are the likely candidates for the artifact wave packets mentioned above. The authors of the pertinent paper "...expect that exact modelling of the FC factors... would improve the match between experiment and theory...",[6] and we suppose that finding a method of separating out the redundant coherences might be the first step in that direction.

4. CONCLUSIONS

An in-depth understanding of singlet fission is a prerequisite for inventing cheaper and more effective light-harvesting devices. The recently designed sophisticated computational technologies[6,19] are paving the way in that direction, yet their complexity and the numerical effort they involve make it inevitable to simplify their underlying physical models. In view of some treacherous subtleties of quantum chemistry calculations of the requisite FC parameters for triplet electronic states, replacing the latter by their singlet counterparts is a tempting simplification. We have shown in the present paper that although this approximation is widely practiced it is risky for subtle interpretative issues of femtosecond pump−probe vibrational spectroscopy where a slight difference in a mode's coherence power might be decisive for the understanding of fission dynamics.

However, the insight we have attained by studying the coherent wave packets induced in TIPS-pentacene and pentacene, viewed as model compounds, seems to suggest that the validity range where the "truncated" approach (with the above replacement made) retains qualitative correctness is (to our surprise) reasonably wide, with only isolated modes that develop into spurious wave packets. In our opinion, this is a vital observation for modern state-of-the-art TTNS calculations of the fission process (like those of refs 6 and 19), which operate in the Hilbert space of 10^{500} states. Then, in view of the computational effort involved, the "exact modelling of the resonance-specific Franck-Condon factors"[6] is too demanding, whereas truncation of their set (in the spirit of our usage of the term) allows one to focus on other aspects of the underlying physics. The first correction that could be introduced into that model might consist in finding a method to identify the singular modes mentioned above and eliminating the redundant signals from the calculated coherence power spectrum.

According to our present experience, the spurious coherences derive from the precursor wave packets that in the truncated model emerge as allowed but are not genuine, i.e., in the complete model they develop into forbidden ones (in the sense of the soft selection rules), so their intensities turn out to be negligible. With FC parameters for the triplet manifold accessible to moderate scale quantum chemistry calculations, the coherence flow descriptors (which are relatively easy to generate) should allow one to pinpoint the redundant coherences with reasonable probability. We hope

https://dx.doi.org/10.1021/acs.jpcc.0c06504
J. Phys. Chem. C 2020, 124, 23501−23510

that a feasible approach to that end will be developed in the future.

■ ASSOCIATED CONTENT

Supporting Information

The Supporting Information is available free of charge at https://pubs.acs.org/doi/10.1021/acs.jpcc.0c06504.

Documentation of the TDDFT calculations (excitation energies and atomic positions for the relevant electronic states), recapitulation of the model and main formulas (derived in earlier papers cited herein) required to repeat the calculations of this paper (PDF)

■ AUTHOR INFORMATION

Corresponding Author

Piotr Petelenz − *The K. Gumiński Department of Theoretical Chemistry, Faculty of Chemistry, Jagiellonian University, 30-387 Kraków, Poland;* orcid.org/0000-0001-5481-1958; Phone: +48 12 6862375; Email: petelenz@chemia.uj.edu.pl

Authors

Marcin Andrzejak − *The K. Gumiński Department of Theoretical Chemistry, Faculty of Chemistry, Jagiellonian University, 30-387 Kraków, Poland;* orcid.org/0000-0002-1798-7249

Grzegorz Mazur − *Department of Computational Methods in Chemistry, Jagiellonian University, 30-387 Kraków, Poland;* orcid.org/0000-0001-7204-1926

Tomasz Skóra − *Department of Complex Systems, Institute of Physical Chemistry, Polish Academy of Sciences, 01-224 Warszawa, Poland;* orcid.org/0000-0003-4394-4928

Complete contact information is available at: https://pubs.acs.org/10.1021/acs.jpcc.0c06504

Notes

The authors declare no competing financial interest.

■ ACKNOWLEDGMENTS

The authors express their gratitude to Andrew Musser for providing the emission spectrum of the pump used in the experiments of ref 10 and for illuminating comments on femtosecond laser spectroscopy. Many thanks are also due to James Hooper for checking the English of the manuscript after the reviews, combined with valuable linguistic comments and phrasing suggestions. This research was performed with equipment purchased owing to the financial support of the European Regional Development Fund in the framework of the Polish Innovation Economy Operational Program (contract no. POIG.02.01.00-12-023/08). It was also supported in part by PL-Grid Infrastructure, with the calculations performed on Prometheus: the Cluster Platform of the Academic Computer Centre CYFRONET.

■ REFERENCES

(1) Smith, M. B.; Michl, J. Recent Advances in Singlet Fission. *Annu. Rev. Phys. Chem.* **2013**, *64*, 361−386.

(2) Miyata, K.; Kurashige, Y.; Watanabe, K.; Sugimoto, T.; Takahashi, S.; Tanaka, S.; Takeya, J.; Yanai, T.; Matsumoto, Y. Coherent Singlet Fission Activated by Symmetry Breaking. *Nat. Chem.* **2017**, *9*, 983−989.

(3) Dron, P. I.; Michl, J.; Johnson, J. C. Singlet Fission and Excimer Formation in Disordered Solids of Alkyl-Substituted 1,3-Diphenylisobenzofurans. *J. Phys. Chem. A* **2017**, *121*, 8596−8603.

(4) Broch, K.; Dieterle, J.; Branchi, F.; Hestand, N. J.; Olivier, Y.; Tamura, H.; Cruz, C.; Nichols, V. M.; Hinderhofer, A.; Beljonne, D.; et al. Robust Singlet Fission in Pentacene Thin Films with Tuned Charge Transfer Interactions. *Nat. Commun.* **2018**, *9*, 954.

(5) Buchanan, E. A.; Michl, J. Packing Guidelines for Optimizing Singlet Fission Matrix Elements in Noncovalent Dimers. *J. Am. Chem. Soc.* **2017**, *139*, 15572−15575.

(6) Schnedermann, C.; Alvertis, A. M.; Wende, T.; Lukman, S.; Feng, J.; Schroder, F. A. Y. N.; Turban, D. H. P.; Wu, J.; Hine, N. D. M.; Greenham, N. C.; et al. A Molecular Movie of Ultrafast Singlet Fission. *Nat. Commun.* **2019**, *10*, 4207.

(7) Hetzer, C.; Guldi, D. M.; Tykwinski, R. R. Pentacene Dimers as a Critical Tool for the Investigation of Intramolecular Singlet Fission. *Chem. - Eur. J.* **2018**, *24*, 8245−8257.

(8) Buchanan, E. A.; Kaleta, J.; Wen, J.; Lapidus, S. H.; Císařová, I.; Havlas, Z.; Johnson, J. C.; Michl, J. Molecular Packing and Singlet Fission: The Parent and Three Fluorinated 1,3-Diphenylisobenzofurans; *J. J. Phys. Chem. Lett.* **2019**, *10*, 1947−1953.

(9) Alvertis, M. A.; Lukman, S.; Hele, T. J. H.; Fuemmeler, E. G.; Feng, J.; Wu, J.; Greenham, N. C.; Chin, A. W.; Musser, A. J. Switching between Coherent and Incoherent Singlet Fission via Solvent Induced Symmetry-Breaking. *J. Am. Chem. Soc.* **2019**, *141*, 17558−17570.

(10) Musser, A. J.; Liebel, M.; Schnedermann, C.; Wende, T.; Kehoe, T. B.; Rao, A.; Kukura, P. Evidence for Conical Intersection Dynamics Mediating Ultrafast Singlet Exciton Fission. *Nat. Phys.* **2015**, *11*, 352−359.

(11) Stern, H. L.; et al. Vibronically Coherent Ultrafast Triplet-Pair Formation and Subsequent Thermally Activated Dissociation Control Efficient Endothermic Singlet Fission. *Nat. Chem.* **2017**, *9*, 1205−1212.

(12) Andrzejak, M.; Skóra, T.; Petelenz, P. Is Vibrational Coherence a Byproduct of Singlet Exciton Fission? *J. Phys. Chem. C* **2019**, *123*, 91−101.

(13) Andrzejak, M.; Skóra, T.; Petelenz, P. Limitations of Generic Chromophore Concept for Femtosecond Vibrational Coherences. *J. Phys. Chem. C* **2020**, *124*, 3529−3535.

(14) Bakulin, A. A.; Morgan, S. E.; Kehoe, T. B.; Wilson, M. W. B.; Chin, A. W.; Zigmantas, D.; Egorova, D.; Rao, A. Real-Time Observation of Multiexcitonic States in Ultrafast Singlet Fission Using Coherent 2D Electronic Spectroscopy. *Nat. Chem.* **2016**, *8*, 16−23.

(15) Tempelaar, R.; Reichman, D. R. Vibronic Exciton Theory of Singlet Fission. II. Two-Dimensional Spectroscopic Detection of the Correlated Triplet Pair State. *J. Chem. Phys.* **2017**, *146*, 174704.

(16) Pabst, M.; Köhn, A. Implementation of Transition Moments Between Excited States in the Approximate Coupled-Cluster Singles and Doubles Model. *J. Chem. Phys.* **2008**, *129*, 214101.

(17) Andrzejak, M.; Petelenz, P. Vibronic Relaxation Energies of Acene-Related Molecules upon Excitation or Ionization. *Phys. Chem. Chem. Phys.* **2018**, *20*, 14061−14071.

(18) *TURBOMOLE*, V6.4; University of Karlsruhe and Forschungszentrum Karlsruhe GmbH and TURBOMOLE GmbH, 2011. http://www.turbomole.com.

(19) Schröder, F. A. J. N.; Turban, D. H. P.; Musser, A. J.; Hine, N. D. M.; Chin, A. W. Tensor Network Simulation of Multi-Environmental Open Quantum Dynamics via Machine Learning and Entanglement Renormalization. *Nat. Commun.* **2019**, *10*, 1062.